

Anomalous resilient to decoherence macroscopic quantum superpositions generated by universally covariant optimal quantum cloning

Nicolò Spagnolo,¹ Fabio Sciarrino,^{1,2} and Francesco De Martini^{1,3}

¹*Dipartimento di Fisica, "Sapienza" Università di Roma and Consorzio Nazionale Interuniversitario per le Scienze Fisiche della Materia, Roma, piazzale Aldo Moro 5, I-00185 Italy*

²*Istituto Nazionale di Ottica Applicata, largo Fermi 6, I-50125 Firenze, Italy*

³*Accademia Nazionale dei Lincei, via della Lungara 10, I-00165 Roma, Italy*

We show that the quantum states generated by universal optimal quantum cloning of a single photon represent an universal set of quantum superpositions resilient to decoherence. We adopt Bures distance as a tool to investigate the persistence of quantum coherence of these quantum states. According to this analysis, the process of universal cloning realizes a class of quantum superpositions that exhibits a covariance property in lossy configuration over the complete set of polarization states in the Bloch sphere.

PACS numbers:

I. INTRODUCTION

In recent years two fundamental aspects of quantum mechanics have attracted a great deal of interest, namely the investigation on the irreducible nonlocal properties of Nature implied by quantum entanglement and the physical realization of the "Schrödinger Cat paradox". The last concept, by applying the nonlocality property to a combination of a microscopic and of a macroscopic systems, enlightens the concept of the quantum state, the dynamics of large systems and ventures into the most intriguing philosophical problem, i.e. the emergence of quantum mechanics in the real life [1]. Unfortunately it was always found extremely difficult to realize a system which realizes simultaneously the following properties of the Schrödinger Cat, i.e. a Micro - Macroscopic Quantum Superposition (MMQS): (a) the quantum superposition of two multiparticle, mutually orthogonal states, call it the "Macro-system" (b) the entanglement of this superposition with a far apart single-particle state, i.e. the "Micro-system". In addition, it was always found that the quantum properties of any realized MMQS scheme were quickly spoiled by the pervasive interactions with the environment: i.e. by the effect of "decoherence", the phase-disrupting effect that so far has impaired the realization of the "quantum computer" [2]. The last crucial drawback made so far still more paradoxical any MMQS scheme. Recently a MMQS realizing the conditions a) and b), consisting of $N \approx 3.5 \times 10^4$ photons in a quantum superposition and entangled with a far apart single-photon state was generated [3]. The structure of this system was realized by means of the quantum-injected optical parametric amplification (QI-OPA), i.e. a optimal quantum-cloning machine. In addition and most surprisingly, our QI-OPA system exhibited an anomalous large resilience to decoherence.

In the present paper we demonstrate that the QI-OPA based MMQS is indeed a "decoherence - free" system which, in particular, is totally insensitive to temperature effects. This makes the device an ideal approach to en-

lighten the quantum-to-classical transition and to investigate the persistence of quantum phenomena into the "classical" domain by measurement procedures applied to quantum systems of increasing size [2]. Furthermore, since the generated Micro-Macro state is directly accessible at the output of the apparatus, the implementation of significant multi qubit logic gates for quantum information technology can be achieved by this method.

About ten years ago it was proposed to exploit the process of quantum cloning to generate a different class of multiphoton states: Fig.1[6, 7]. This method led recently to the successful experimental realization of an entangled macroscopic quantum superposition (MQS) of a large number of particles $N \approx 5 \times 10^4$ [3, 8]. The persistence of quantum coherence in MQS states realized by the "phase-covariant" cloning, i.e. limited to a *one dimensional* subspace of the entire Bloch sphere of the Macro-qubit was analyzed on the basis of two criteria based on the definition of "distance" in the Hilbert space [9, 10]. It was found that that limited physical system shows a high resilience to decoherence at variance with any coherent $|\alpha\rangle$ state MQS. The nice feature of phase-covariance symmetry mostly consists of the relative simplicity of the required "collinear" structure and of the high efficiency of the QI-OPA. This one amplifies equally well all the single-photon polarization states $|\phi\rangle$ belonging to the equatorial plane of the Bloch sphere of the injected micro-qubit [7, 8].

Given that lucky circumstance, a question arose whether it exists a physical systems that exhibits the property of *decoherence - freedom* in a larger Hilbert space or, better, in the *full space* available to the generated Macrostate. The answer is yes, as demonstrated in the present paper. The "*universal quantum cloning machine*" realized in its "*optimal*" MMQS mode non-degenerate configuration indeed possesses the requested property: the *decoherence - freedom* is realized in the *full Hilbert space* spanned by the output Macrostate [6, 11–13].

In this paper, we report the theoretical analysis on the resilience to decoherence of the quantum states generated

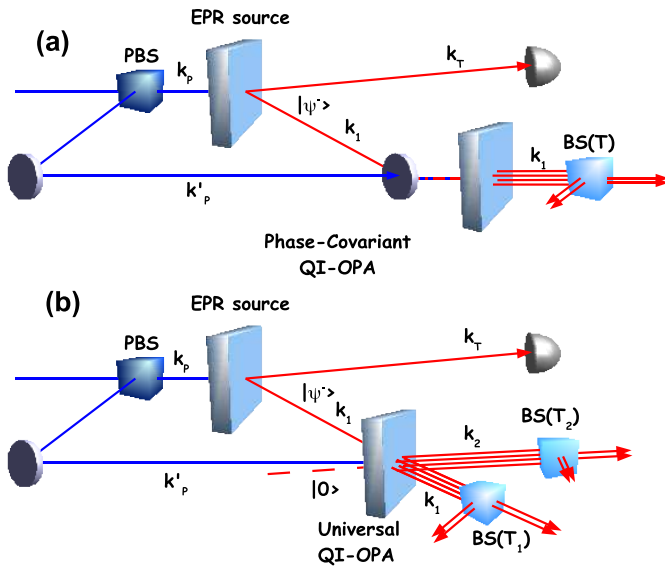


FIG. 1: (a) Scheme for the phase-covariant cloning of a single photon state with a non-collinear optical parametric amplifier. The beam-splitter [BS(T)] is inserted to simulate the propagation over lossy channels of the output field. (b) Scheme for the universal cloning of a single photon state with a non-collinear optical parametric amplifier (beam-splitters on spatial modes \mathbf{k}_1 [BS(T_1)] and \mathbf{k}_2 [BS(T_2)]).

by universal quantum cloning of a single-photon qubit. The basic tools of this investigation are provided by the two coherence criteria defined in Refs. [9, 10]. There, the Bures distance [14–16]:

$$\mathcal{D}(\hat{\rho}, \hat{\sigma}) = \sqrt{1 - \sqrt{\mathcal{F}(\hat{\rho}, \hat{\sigma})}}, \quad (1)$$

where \mathcal{F} is a quantum “fidelity”, has been adopted as a measure to quantify: (I) the “*distinguishability*” between two quantum states $\{|\phi_1\rangle, |\phi_2\rangle\}$ and (II) the *degree of coherence*, i.e. MQS visibility, of their quantum superpositions $|\phi^\pm\rangle = 2^{-1/2}(|\phi_1\rangle \pm |\phi_2\rangle)$. These criteria were chosen according to the following considerations. (I) The distinguishability i.e. the degree of orthogonality, represents the maximum discrimination power among two quantum states available within a measurement. (II) The related “*Visibility*” between the superpositions $|\phi^+\rangle$ and $|\phi^-\rangle$ depends exclusively on the relative phase of the component states: $|\phi_1\rangle$ and $|\phi_2\rangle$. Consider two orthogonal superpositions $|\phi^\pm\rangle$: $\mathcal{D}(|\phi^+\rangle, |\phi^-\rangle) = 1$. In presence of decoherence the relative phase between $|\phi_1\rangle$ and $|\phi_2\rangle$ progressively randomizes and the superpositions $|\phi^+\rangle$ and $|\phi^-\rangle$ approach an identical fully mixed state leading to: $\mathcal{D}(|\phi^+\rangle, |\phi^-\rangle) = 0$. The physical interpretation of $\mathcal{D}(|\phi^+\rangle, |\phi^-\rangle)$ as “*Visibility*” of a superposition $|\phi^\pm\rangle$ is legitimate insofar as the component states of the corresponding superposition, $|\phi_1\rangle$ and $|\phi_2\rangle$ may be defined, at least approximately, as “*pointer states*” or “*elected states*” [2]. Within the set of the eigenstates characterizing any quantum system the pointer states are de-

finied as the ones least affected by the external noise and that are highly resilient to decoherence. In other words, the pointer states are “quasi classical” states which realize the minimum flow of information from (or to) the System to (or from) the Environment. They are involved in all criteria of classicality, such as the ones based on “purity” and “predictability” of the macrostates [2].

Our interest is aimed at the resilience properties of the different classes of quantum states after the propagation over a lossy channel. This one is modelled by a linear beam-splitter (BS) with transmittivity T and reflectivity $R = 1 - T$ acting on a state $\hat{\rho}$ associated with a single BS input mode: Fig.1. Let us first analyze the behaviour of the coherent states and their superpositions. The investigation on the Glauber’s states leading to the α -MQS’s case [4]: $|\Phi_{\alpha\pm}\rangle = \mathcal{N}^{-1/2}(|\alpha\rangle \pm |-\alpha\rangle)$ in terms of the “pointer states” $|\pm\alpha\rangle$ leads to the closed form result: $\mathcal{D}(|\Phi_{\alpha+}\rangle, |\Phi_{\alpha-}\rangle) = \sqrt{1 - \sqrt{1 - e^{-4R}|\alpha|^2}}$. This one is plotted in Fig.2 (dashed line) as function of the average number of lost photons: $x \equiv R\langle n \rangle$. Note that the value of $\mathcal{D}(|\Phi_{\alpha+}\rangle, |\Phi_{\alpha-}\rangle)$ drops from 1 to 0.095 upon loss of only one photon: $x = 1$. In other words, the superpositions of α -states. $|\Phi_{\alpha\pm}\rangle = \mathcal{N}^{-1/2}(|\alpha\rangle \pm |-\alpha\rangle)$ exhibit a fast decrease in their coherence, i.e. of their “visibility” and “distinguishability”, while the related components $|\pm\alpha\rangle$, i.e. the “pointer states” [2], remain distinguishable until all photons of the state are depleted by the BS.

The amplification QI-OPA systems under investigation are reported in Fig.1. An EPR pair $|\psi^-\rangle = 2^{-1/2}(|H\rangle_1|V\rangle_T - |V\rangle_1|H\rangle_T)$ is generated in a first non-linear crystal. The symbols H and V refer to horizontal and vertical field polarizations, i.e. the extreme “poles” of the Poincaré sphere. By analyzing and measuring the polarization of the photon associated with the mode \mathbf{k}_T , the photon on mode \mathbf{k}_1 is nonlocally prepared in the polarization qubit: $|\psi\rangle_1 = \cos(\theta/2)|H\rangle_1 + e^{i\phi}\sin(\theta/2)|V\rangle_1$. Then, by an accurate spatial focusing the single photon in the state $|\psi\rangle_1$ is injected in the amplifier simultaneously with the strong UV pump beam \mathbf{k}'_P . Let us analyze the two configurations of the apparatus leading, as said, to two different regimes of quantum cloning: the “phase covariant” and the “universal”.

II. PHASE-COVARIANT OPTIMAL QUANTUM CLONING MACHINE

Let us first briefly review the results obtained for a “collinear” optical configuration, i.e. leading to the phase-covariant optimal quantum cloning machine: Figure 1 (a). The interaction Hamiltonian of this process is: $\hat{\mathcal{H}}_{PC} = i\hbar\chi\hat{a}_H^\dagger\hat{a}_V^\dagger + \text{H.c.}$ in the $\{\pi_H, \pi_V\}$ polarization basis, and $\hat{\mathcal{H}}_{PC} = \frac{i\hbar\chi}{2}e^{-i\phi}(\hat{a}_\phi^{\dagger 2} - e^{i2\phi}\hat{a}_{\phi\perp}^{\dagger 2}) + \text{H.c.}$ for any “equatorial” basis $\{\pi_\phi, \pi_{\phi\perp}\}$ on the Poincaré sphere having as “poles” the states: π_H, π_V . The relevant equatorial basis considered here are $\{\pi_+, \pi_-\}$ and $\{\pi_R, \pi_L\}$ corresponding respectively to $\phi = 0$ and $\phi = \pi/2$. The

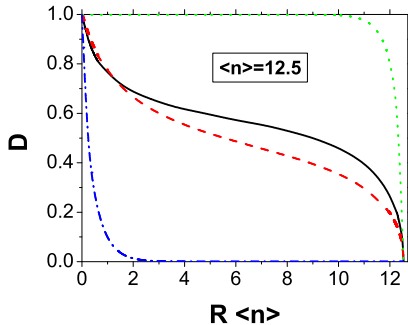


FIG. 2: Bures distance for various classes of MQSs for $\langle n \rangle = 12.5$. The lower blue dash-dotted curve corresponds to the quantum superpositions of coherent states $|\alpha\rangle \pm |-\alpha\rangle$, while the green dotted upper curve is relative to the distinguishability between the component states $|\pm\alpha\rangle$. The black straight curve corresponds to the MQS generated by phase-covariant cloning [9, 10], while the red dashed curve corresponds to the universal cloning based MQS.

amplified state for an injected equatorial qubit is:

$$|\Phi_{PC}^\phi\rangle = \sum_{i,j=0}^{\infty} \gamma_{ij} |(2i+1)\phi, (2j)\phi_\perp\rangle \quad (2)$$

where $\gamma_{ij} = \frac{1}{C^2} (e^{-\nu\varphi} \frac{\Gamma}{2})^i (-e^{\nu\varphi} \frac{\Gamma}{2})^j \frac{\sqrt{(2i+1)!} \sqrt{(2j)!}}{i!j!}$, $C = \cosh g$, $\Gamma = \tanh g$. Hereafter, $|p\psi, q\psi_\perp\rangle_i$ stands for a Fock state with p photons polarized $\vec{\pi}_\psi$ and q photons polarized $\vec{\pi}_{\psi_\perp}$ on spatial mode \mathbf{k}_i . We evaluated numerically the *distinguishability* of $\{|\Phi_{PC}^{\pm}\rangle\}$ through the distance $\mathcal{D}(|\Phi_{PC}^+\rangle, |\Phi_{PC}^-\rangle)$: Fig.2. Consider the MQS of the macrostates $|\Phi_{PC}^+\rangle$, $|\Phi_{PC}^-\rangle$: $|\Psi_{PC}^\pm\rangle = \frac{N_\pm}{\sqrt{2}} (|\Phi_{PC}^+\rangle \pm i|\Phi_{PC}^-\rangle)$. Due to the linearity of the amplification process [11], $|\Psi_{PC}^\pm\rangle = |\Phi_{PC}^{R/L}\rangle$ and in virtue of the phase-covariance of the process:

$$\mathcal{D}(|\Psi_{PC}^+\rangle, |\Psi_{PC}^-\rangle) = \mathcal{D}(|\Phi_{PC}^R\rangle, |\Phi_{PC}^L\rangle) = \mathcal{D}(|\Phi_{PC}^+\rangle, |\Phi_{PC}^-\rangle) \quad (3)$$

These equations can be assumed as the theoretical conditions assuring the *decoherence - freedom* of any quantum MMQS state generated by the QI-OPA in the collinear configuration: they identify the "equatorial set" of the Bloch sphere a privileged *decoherence-free* Hilbert subspace. The *visibility* of the q-MQS $\{|\Psi_{PC}^{\pm}\rangle\}$ was evaluated numerically analyzing the Bures distance as a function of x . Note that for small values of x the decay of $D(x)$ is far slower than for the coherent $\alpha - MQS$ case. This resilience to decoherence feature has been experimentally verified in [3].

III. UNIVERSAL OPTIMAL QUANTUM CLONING MACHINE

Let's now investigate the resilience to decoherence of the MMQS generated by the *universal optimal quantum*

cloning machine (UOQCM). According to the original proposal, this was implemented experimentally by QI-OPA device working in a non-collinear, i.e. mode non-degenerate configuration: Figure 2 (b) [6]. This parametric amplifier acts as an universal $N \rightarrow M$ quantum cloning machine [17, 18] as well as a *Universal - Not* (U-Not) quantum machine [19]. The interaction Hamiltonian for the amplifier is now given by $\hat{H}_U = i\hbar\chi(\hat{a}_{1\psi}^\dagger \hat{a}_{2\psi_\perp}^\dagger - \hat{a}_{1\psi_\perp}^\dagger \hat{a}_{2\psi}^\dagger) + \text{H.c.}$, where $\vec{\pi}_\psi = \cos(\theta/2)\vec{\pi}_H + e^{i\phi} \sin(\theta/2)\vec{\pi}_V$ and $\vec{\pi}_{\psi_\perp} = (\vec{\pi}_\psi)^\perp$. Since this system possesses a complete SU(2) symmetry, the Hamiltonian maintains the same form for any simultaneous rotation of the Bloch sphere of the polarization basis for both output modes \mathbf{k}_1 and \mathbf{k}_2 .

The output state of the amplifier reads:

$$|\Phi_U^{1\psi}\rangle = \hat{U}|1\psi\rangle_1 = \frac{1}{C^3} \sum_{n,m=0}^{\infty} \Gamma^{n+m} (-1)^m \sqrt{n+1} \quad (4)$$

$$|(n+1)\psi, m\psi_\perp\rangle_1 \otimes |m\psi, n\psi_\perp\rangle_2$$

In order to investigate the features of the state of Eq.(4), Fig.3 reports the photon-number distribution for the reduced states $\hat{\rho}_{U\mathbf{k}_i}^{1\psi(1\psi_\perp)} = \text{Tr}_{\mathbf{k}_i} [|\Phi_U^{1\psi(1\psi_\perp)}\rangle\langle\Phi_U^{1\psi(1\psi_\perp)}|]$ associated to the output spatial modes \mathbf{k}_1 and \mathbf{k}_2 . The photon-number distributions in the \mathbf{k}_1 spatial mode [Figs.3-(a) and (c)], i.e. the cloning mode, show a strong unbalancement along the direction of the injected polarization state. The anticloning \mathbf{k}_2 mode [Figs.3-(b) and (d)] presents the opposite unbalancement along the direction of the orthogonal polarization, since on that spatial mode the amplifier works as a *U-Not machine* [19]. This feature is also enlightened by the contour plots of Figs.3-(e-h), where the white regions represent the Fock-space zones where the photon-number distributions are more densely populated. Furthermore, we note that at variance with the phase-covariant amplifier [9, 10], the output states do not exhibit any comb structure in their photon number distributions. In agreement with the "universality" property of the source, the Bures distance between the MQS states $|\Phi_U^{1\psi}\rangle = \cos(\theta/2)|\Phi_U^{1H}\rangle + e^{i\phi} \sin(\theta/2)|\Phi_U^{1V}\rangle$ and $|\Phi_U^{1\psi_\perp}\rangle$ is independent on the choice of (θ, ϕ) :

$$\mathcal{D}(\hat{\rho}_U^{1\psi}, \hat{\rho}_U^{1\psi_\perp}) = \mathcal{D}(\hat{\rho}_U^{1\psi'}, \hat{\rho}_U^{1\psi'_\perp}) \quad (5)$$

for any basis $\{\vec{\pi}_\psi, \vec{\pi}_{\psi'}\}$. This feature is the extension of the ϕ -covariance property of the collinear quantum cloning machine [10] to the full set of polarization states on the output Bloch spheres..

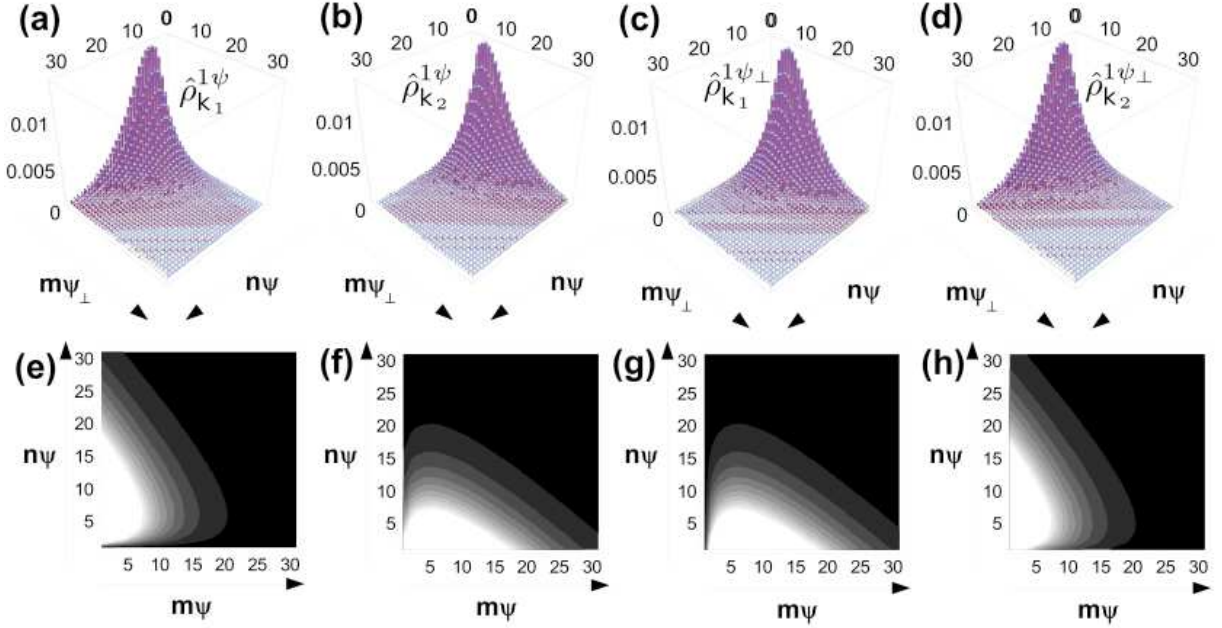


FIG. 3: Probability distribution (a-d) and contour plots (e-h) of the reduced density matrices $\hat{\rho}_{\mathbf{k}_1}^{1\psi}$ (a)-(e), $\hat{\rho}_{\mathbf{k}_2}^{1\psi}$ (b)-(f), $\hat{\rho}_{\mathbf{k}_1}^{1\psi\perp}$ (c)-(g) and $\hat{\rho}_{\mathbf{k}_2}^{1\psi\perp}$ (d)-(h). All plots correspond to the gain value $g = 1.5$.

By introducing, in analogy with the previous case, two beam-splitters (BS_1 and BS_2) on the output states, we evaluate by standard algebraic numerical routines the Bures distance between the orthogonal macrostates $|\Phi_U^{1\psi}\rangle$ and $|\Phi_U^{1\psi\perp}\rangle$ as a functions of the corresponding transmission parameters: T_1 and T_2 . In Fig.4-(a) we report the 3-dimensional plot of the function $\mathcal{D}(R_1, R_2) = \mathcal{D}(\hat{\rho}^{1\psi}, \hat{\rho}^{1\psi\perp})$ for a gain value of $g = 1.2$, corresponding to an overall average number of photons $\langle \hat{n} \rangle = \sum_{i=1}^2 [\langle \hat{n}_{i\psi} \rangle + \langle \hat{n}_{i\psi\perp} \rangle] \approx 15$. The Figure shows that the MQS visibility possesses a resilient structure in presence of losses, since the Bures distance does not decrease exponentially with the lossy parameters $\{R_1, R_2\}$. In Figs.4-(b-c) we then report several sections of the 3-dimensional surface of Fig.4-(a) by fixing either R_1 or R_2 . We note that the $|\Phi_U^{1\psi}\rangle$ and $|\Phi_U^{1\psi\perp}\rangle$ MQSs are more sensitive to losses in the *cloning* mode: \mathbf{k}_1 than in the *anticloning* one: \mathbf{k}_2 . This can be explained by considering that the distance between these orthogonal Macrostates depends on the unbalancement in the corresponding photon-number distributions. Since this feature is pronounced in the spatial cloning mode \mathbf{k}_1 , losses acting on this mode cancel more rapidly the orthogonality between $|\Phi_U^{1\psi}\rangle$ and $|\Phi_U^{1\psi\perp}\rangle$. As the number of photons present in the state is increased, the visibility keeps large up to a value $V \approx 0.5$ in a larger range of the number of reflected photons. All this shows that, in analogy with the phase-covariant case, the MQS's generated by quantum cloning become more resilient to losses since the quantum coherence present in these state can survive the loss of a larger number of photons.

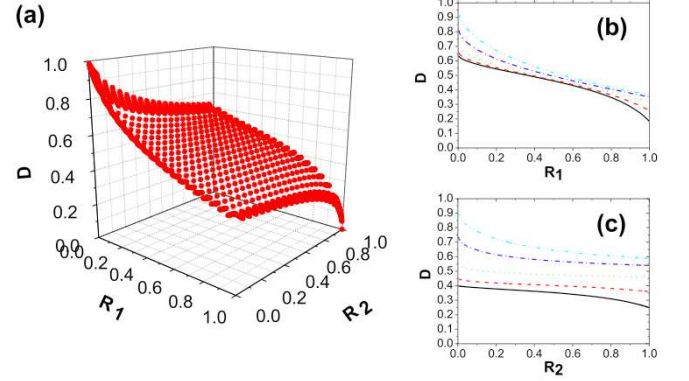


FIG. 4: Bures distance between the MQSs $|\Phi_U^{1\psi}\rangle$ and $|\Phi_U^{1\psi\perp}\rangle$ after losses. (a) 3-dimensional surface $\mathcal{D}(R_1, R_2)$ as a function of the two spatial mode parameters $R_1 = 1 - T_1$ and $R_2 = 1 - T_2$. (b) $\mathcal{D}(R_1, R_2)$ with R_2 fixed, as a function of R_1 . (c) $\mathcal{D}(R_1, R_2)$ with R_1 fixed, as a function of R_2 . (b)-(c) Straight curves correspond to $R_{2(1)} = 0.9$, the dashed curves to $R_{2(1)} = 0.75$, dotted one to $R_{2(1)} = 0.5$, the dash-dotted curves to $R_{2(1)} = 0.2$ and dash-dot-dotted curves to $R_{2(1)} = 0.05$.

Finally we analyze the action of the Orthogonality Filter (O-Filter, OF) on the amplified single photon states $|\Phi_U^{1\psi}\rangle$ by analyzing how the Bures distance is affected by the application of this device. The POVM like technique [20] implied by this device locally selects the events for which the difference between the photon numbers associated with two orthogonal polarizations $|m - n| > k$,

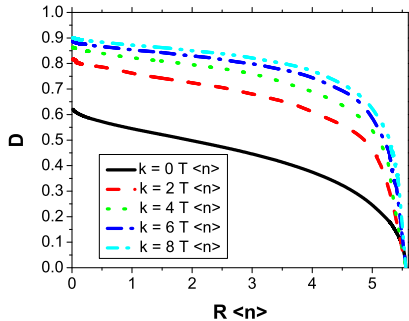


FIG. 5: Numerical results for the Bures distance between the $|\Phi^{1\psi}\rangle$ and $|\Phi^{1\psi\perp}\rangle$ states after the propagation over a lossy channel and the application of the O-Filter device. From the lower to the upper curve, the filtering threshold is set to $k = 0\langle n \rangle$ ($P_{filt} = 1$), $k = 2\langle n \rangle$ ($P_{filt} = 1.7 \times 10^{-1}$), $k = 4\langle n \rangle$ ($P_{filt} = 1.5 \times 10^{-2}$), $k = 6\langle n \rangle$ ($P_{filt} = 1.1 \times 10^{-3}$), $k = 8\langle n \rangle$ ($P_{filt} = 8.2 \times 10^{-5}$). All curves are calculated for a gain $g = 1.2$, corresponding to an average number of generated photons on mode \mathbf{k}_1 equal to $\langle n \rangle \simeq 8$.

i.e. larger than an adjustable threshold, k [8]. By this method a sharper discrimination between the output states $|\Phi_U^{1\psi}\rangle$ and $|\Phi_U^{1\psi\perp}\rangle$ can be achieved. We focus our attention only on the reduced density matrix $\hat{\rho}_{\mathbf{k}_1}^{1\psi}(T)$ corresponding to the output spatial mode \mathbf{k}_1 . We then applied the numerical methods previously adopted in order to calculate the Bures distance $\mathcal{D}(x)$, where $x = R\langle n \rangle$ is the number of lost photons, as a function of the threshold k . In Fig.5 the results of a numerical analysis carried out for $g = 1.2$ and different values of k are reported.

Note the increase of the value of $\mathcal{D}(x)$, i.e. of the MQS Visibility, by increasing k . Of course, in the spirit of any POVM measurement, the high interference visibility is here achieved at the cost of a lower success probability [21]. The general, most important feature shown by all these Figures is that both the “*Distinguishability*” and the “*Visibility*” of all “universal” macrostates $|\Phi_U^{1\psi}\rangle, |\Phi_U^{1\psi\perp}\rangle$ as well as of all their “universal” quantum superpositions can be kept close to the maximum value in spite of the increasing effect of decoherence due to increasing values of the BS_1 reflectivity: $R\langle n \rangle$. On the basis of all these results we may then conclude that all the “universal” macrostates and superpositions generated by the QI-OPA may be safely defined as classically stable, *inselected “pointer states”* [2].

IV. CONCLUSIONS

The present paper reports a thorough theoretical analysis on the resilience to decoherence of the quantum superpositions generated by universal quantum cloning. This property is found to depend on the symmetry (“co-variance”) of the optimal cloning process, which allows

to identify a covariant set of stable quantum superpositions over the full Hilbert space spanned by the generated Macro-states. In order to gain insight into the general picture and to support the congruence of our final conclusions we find useful to relate here the various aspects of the optimal cloning process with the current MQS physical model considered by [2].

1) The “*System*” in our optical entangled amplification scheme is represented by the assembly of $N + 1$ photon particles associated with the macrostate $|\Phi^\phi\rangle$ generated by the optimal cloning apparatus.

2) The flow of (classical) “noise information” directed from the “*Environment*” towards the *System* is attributed to the unavoidable squeezed-vacuum noise affecting the building up of the macrostate $|\Phi^\phi\rangle$ within the process of amplification. As already stressed, the “*optimality*” of the quantum cloning generally implies that the flow of classical noise is the *minimum* allowed by the principles of quantum mechanics, i.e. by the “*no-cloning theorem*” [22, 23].

3) The flow of quantum information directed from the System towards the Environment is provided by the controlled “decoherence in action” provided by the BS-scattering process and by the losses taking place in all photo-detection processes. We have seen that by the use of the OF, or even in the absence of it, the interference phase-distrupting effects caused by the decoherence can be efficiently tamed for the macrostates and for their quantum superpositions.

4) By the universal cloning method considered here the maximum allowed *Distinguishability* and *Visibility* are attained for the macro-qubit Hilbert space.

5) In any cloning apparatus a unitary transformation \hat{U} connects all physical properties belonging to the micro-world to the corresponding ones belonging to the macroscopic “classical” world. Any lack of perceiving this close correspondence, for instance in connection with the realization of the “Schrödinger Cat” must be only attributable to the intrinsic limitations of our perceiving senses, of our observational methods or of our measurement apparatus. In other words, at least in our case, the two worlds are deterministically mirrored one into the other by the unitary map \hat{U} which is provided by quantum mechanics itself. This is the key to understand our results.

6) The q-MQS based on the cloning process is not a “thermodynamic” system as its dynamics and decoherence do not depend on the temperature T . It rather belongs to, and indeed establishes a first and most insightful physical model of, the class of the “*parametrically - driven, open quantum - statistical systems*” that have been recently invoked to provide and sustain extended long - range nonlocal coherence processes in complex biological photosynthetic systems [24, 25]

Appendix A: Calculation of the density matrix coefficients for the universally amplified single-photon states in presence of losses

In this appendix we report the detailed calculation of the coefficient of the density matrix for the $|\Phi^{1\psi}\rangle$ states in presence of losses. We focus our attention on the $|1\psi\rangle_1$ case only, since the calculation for the complementary state $|1\psi_\perp\rangle_1$ is similar.

First we investigate the features of the interaction Hamiltonian. Due to the properties of $\hat{\mathcal{H}}_U$, the time evolution operator in the interaction picture $\hat{U} = \exp(-i\hat{\mathcal{H}}_U t/\hbar)$ can be decomposed as the product of two independent operators $\hat{U} = \hat{U}_\mathcal{A} \otimes \hat{U}_{\mathcal{A}'}$, acting on two different Hilbert spaces corresponding to the two sets of modes $\mathcal{A} \equiv \{(\mathbf{k}_1, \vec{\pi}_\psi), (\mathbf{k}_2, \vec{\pi}_{\psi_\perp})\}$ and $\mathcal{A}' \equiv \{(\mathbf{k}_1, \vec{\pi}_{\psi_\perp}), (\mathbf{k}_2, \vec{\pi}_\psi)\}$ [17, 18]:

$$\hat{U}_\mathcal{A} = \exp\left[\chi t(\hat{a}_{1\psi}^\dagger \hat{a}_{2\psi_\perp}^\dagger - \hat{a}_{1\psi} \hat{a}_{2\psi_\perp})\right] \quad (\text{A1})$$

$$\hat{U}_{\mathcal{A}'} = \exp\left[-\chi t(\hat{a}_{1\psi_\perp}^\dagger \hat{a}_{2\psi}^\dagger - \hat{a}_{1\psi_\perp} \hat{a}_{2\psi})\right] \quad (\text{A2})$$

In the case of a separable input state in the QI-OPA $\hat{\rho} = \hat{\rho}_\mathcal{A} \otimes \hat{\rho}_{\mathcal{A}'}$, the amplified states can be written in a separable form:

$$\hat{\rho}(t) = \hat{U} \hat{\rho} \hat{U}^\dagger = \left(\hat{U}_\mathcal{A} \hat{\rho}_\mathcal{A} \hat{U}_\mathcal{A}^\dagger\right) \otimes \left(\hat{U}_{\mathcal{A}'} \hat{\rho}_{\mathcal{A}'} \hat{U}_{\mathcal{A}'}^\dagger\right) \quad (\text{A3})$$

This separability property will be exploited in the remaining part of the paper both for the calculation of the density matrix after losses and for the evaluation of the Bures distance.

1. Density matrix coefficients for the amplified states

In this section we derive the density matrix coefficients for the amplified states $|\Phi^{1\psi(1\psi_\perp)}\rangle$ after the transmission over a lossy channel. We focus our attention on the $|1\psi\rangle_1$ case only, since the calculation for the complementary state $|1\psi_\perp\rangle_1$ is similar. Due to the property of the ‘‘universal’’ amplifier analyzed previously, we analyze separately the two subspaces \mathcal{A} and \mathcal{A}' [Eq.(A3)]. Since the time evolution operators $\hat{U}_\mathcal{A}$ and $\hat{U}_{\mathcal{A}'}$ are equivalent apart from a global phase factor (-1) , the quantum states for the amplifier \mathcal{A}' can be directly derived from the expressions obtained for amplifier \mathcal{A} . Only two relevant cases are considered: the vacuum injected state $\hat{U}_\mathcal{A}|0\rangle$ (spontaneous emission) and the single-photon injected $\hat{U}_\mathcal{A}|1\psi\rangle_1$ state. This analysis can be performed separately for the two amplifiers since the separability feature also holds after the amplified state propagates over a lossy channel in both \mathbf{k}_1 and \mathbf{k}_2 spatial modes. This is a consequence

of the properties of the lossy channel map, which being a ‘‘local’’ transformation, acts independently on each mode. The output state after losses reads:

$$\mathcal{L}[\hat{\rho}(t)] = \mathcal{L}_\mathcal{A} \left[\hat{U}_\mathcal{A} \hat{\rho}_\mathcal{A} \hat{U}_\mathcal{A}^\dagger \right] \otimes \mathcal{L}_{\mathcal{A}'} \left[\hat{U}_{\mathcal{A}'} \hat{\rho}_{\mathcal{A}'} \hat{U}_{\mathcal{A}'}^\dagger \right] \quad (\text{A4})$$

Here $\mathcal{L}_\mathcal{A} = \mathcal{L}_{\mathbf{k}_1, \vec{\pi}_\psi} \otimes \mathcal{L}_{\mathbf{k}_2, \vec{\pi}_{\psi_\perp}}$, $\mathcal{L}_{\mathcal{A}'} = \mathcal{L}_{\mathbf{k}_1, \vec{\pi}_{\psi_\perp}} \otimes \mathcal{L}_{\mathbf{k}_2, \vec{\pi}_\psi}$ are the maps induced by losses for the two subspaces, where the single mode map $(\mathbf{k}_i, \vec{\pi})$ is given by the following expression [26]:

$$\mathcal{L}_{\mathbf{k}_i, \vec{\pi}}[\hat{\sigma}] = \sum_{p=0}^{\infty} R_i^{p/2} T_i^{(\hat{a}^\dagger \hat{a})/2} \frac{\hat{a}_{\mathbf{k}_i, \vec{\pi}}^p}{\sqrt{p!}} \hat{\sigma} \frac{\hat{a}_{\mathbf{k}_i, \vec{\pi}}^{\dagger p}}{\sqrt{p!}} T_i^{(\hat{a}^\dagger \hat{a})/2} R_i^{p/2} \quad (\text{A5})$$

with T_i the transmission efficiency of the channel, assumed to be polarization independent.

We begin with the analysis of the spontaneous emission regime. The calculation proceeds as follows. Starting from the quantum state for the subsystem \mathcal{A} $\hat{U}_\mathcal{A}|0\rangle$, the output state after the transmission over the lossy channel is obtained by applying the lossy channel map (A5) to the density matrix of the state $\hat{\rho}_\mathcal{A}^0$. The same procedure applies for the single photon amplified states, where the seed of the amplifier \mathcal{A} is the single photon state $|1\psi\rangle$. In this case, the input state in the lossy channel is $\hat{U}_\mathcal{A}$. By applying the lossy channel map over the density matrix $\hat{\rho}_\mathcal{A}^{1\psi}$ of the state, we find the desired output states. Details on the calculation and the complete expressions of the coefficients for the density matrices $\hat{\rho}_\mathcal{A}^{1\psi}(T_1, T_2)$ and $\hat{\rho}_\mathcal{A}^0(T_1, T_2)$ are reported below.

Let us emphasize that, due to analogy of the Hamiltonian of the two amplifier \mathcal{A} and \mathcal{A}' , the density matrices of the states $\hat{\rho}_{\mathcal{A}'}^0(T_1, T_2)$ and $\hat{\rho}_{\mathcal{A}'}^{1\psi_\perp}(T_1, T_2)$ for amplifier \mathcal{A}' can be directly derived from Eqs.(A8-A10) and (A13-A15) by substituting (Γ) with $(-\Gamma)$ and by relabelling the indexes describing the spatial and polarization modes.

We begin with the analysis of the spontaneous emission regime. The quantum state for the subsystem \mathcal{A} is given by:

$$\hat{U}_\mathcal{A}|0\rangle = \frac{1}{C} \sum_{n=0}^{\infty} \Gamma^n |n\psi\rangle_1 \otimes |m\psi_\perp\rangle_2 \quad (\text{A6})$$

The output state after the transmission over the lossy channel is obtained by applying the lossy channel map (A5) to the density matrix of the state $\hat{\rho}_\mathcal{A}^0$:

$$\hat{\rho}_\mathcal{A}^0(T_1, T_2) = \left(\mathcal{L}_{\mathbf{k}_1, \vec{\pi}_\psi} \otimes \mathcal{L}_{\mathbf{k}_2, \vec{\pi}_{\psi_\perp}} \right) [\hat{\rho}_\mathcal{A}^0] \quad (\text{A7})$$

After direct application of the lossy channel map on the density matrix, the following expression is obtained:

$$\begin{aligned} \hat{\rho}_{\mathcal{A}}^0(T_1, T_2) &= \sum_{i=0}^{\infty} \sum_{j=0}^i \sum_{k=i-j}^{\infty} [\hat{\rho}_{\mathcal{A}}^0(T_1, T_2)]_{ijk}^{(i \geq j)} |i\psi\rangle_1 \langle k\psi| \otimes |j\psi_{\perp}\rangle_2 \langle (j+k-i)\psi_{\perp}| + \\ &+ \sum_{i=0}^{\infty} \sum_{j=i+1}^{\infty} \sum_{k=0}^{\infty} [\hat{\rho}_{\mathcal{A}}^0(T_1, T_2)]_{ijk}^{(i < j)} |i\psi\rangle_1 \langle k\psi| \otimes |j\psi_{\perp}\rangle_2 \langle (j+k-i)\psi_{\perp}| \end{aligned} \quad (\text{A8})$$

where the coefficients for $i \geq j$ and $i < j$ are given by:

$$[\hat{\rho}_{\mathcal{A}}^0(T_1, T_2)]_{ijk}^{(i \geq j)} = \frac{1}{C^2} \Gamma^{i+k} \frac{T_1^{(i+k)/2} T_2^{(2j+k-i)/2} R_2^{i-j} \sqrt{i!k!}}{(i-j)! \sqrt{j!(j+k-i)!}} {}_2F_1(1+i, 1+k, i+i-j; \Gamma^2 R_1 R_2) \quad (\text{A9})$$

$$[\hat{\rho}_{\mathcal{A}}^0(T_1, T_2)]_{ijk}^{(i < j)} = \frac{1}{C^2} \Gamma^{i+k} \frac{T_1^{(i+k)/2} T_2^{(2j+k-i)/2} R_1^{j-i} \sqrt{j!(j+k-i)!}}{(j-i)! \sqrt{i!k!}} {}_2F_1(1+j, 1+j+k-i, 1+j-i; \Gamma^2 R_1 R_2) \quad (\text{A10})$$

where ${}_2F_1(a, b, c; z)$ is the hypergeometric function defined in Ref. [27]. The same procedure has been applied to the stimulated case, where the seed of the amplifier \mathcal{A} is the single photon state $|1\psi\rangle$. In this case, the input state in the lossy channel has the following expression:

$$\hat{U}_{\mathcal{A}}|1\psi\rangle_1 = \frac{1}{C^2} \sum_{n=0}^{\infty} \Gamma^n \sqrt{n+1} |(n+1)\psi\rangle_1 \otimes |m\psi_{\perp}\rangle_2 \quad (\text{A11})$$

By applying the lossy channel map over the density matrix $\hat{\rho}_{\mathcal{A}}^{1\psi}$ of the state, we find:

$$\hat{\rho}_{\mathcal{A}}^{1\psi}(T_1, T_2) = \left(\mathcal{L}_{\mathbf{k}_1, \vec{\pi}_{\psi}} \otimes \mathcal{L}_{\mathbf{k}_2, \vec{\pi}_{\psi_{\perp}}} \right) \left[\hat{\rho}_{\mathcal{A}}^{1\psi} \right] \quad (\text{A12})$$

The application of the map leads to the following expression for the density matrix:

$$\begin{aligned} \hat{\rho}_{\mathcal{A}}^{1\psi}(T_1, T_2) &= \sum_{i=0}^{\infty} \sum_{j=0}^{i-1} \sum_{k=i-j}^{\infty} [\hat{\rho}_{\mathcal{A}}^{1\psi}(T_1, T_2)]_{ijk}^{(i \geq j+1)} |i\psi\rangle_1 \langle k\psi| \otimes |j\psi_{\perp}\rangle_2 \langle (j+k-i)\psi_{\perp}| + \\ &+ \sum_{i=0}^{\infty} \sum_{j=i}^{\infty} \sum_{k=0}^{\infty} [\hat{\rho}_{\mathcal{A}}^{1\psi}(T_1, T_2)]_{ijk}^{(i \geq j)} |i\psi\rangle_1 \langle k\psi| \otimes |j\psi_{\perp}\rangle_2 \langle (j+k-i)\psi_{\perp}| \end{aligned} \quad (\text{A13})$$

where the coefficients for $i \geq j+1$ and $i \leq j$ are given by:

$$[\hat{\rho}_{\mathcal{A}}^{1\psi}(T_1, T_2)]_{ijk}^{(i \geq j+1)} = \frac{1}{C^4} \Gamma^{i+k-2} \frac{T_1^{(i+k)/2} T_2^{(2j+k-i)/2} R_2^{i-j-1} \sqrt{i!k!}}{(i-j-1)! \sqrt{j!(j+k-i)!}} {}_2F_1(1+i, 1+k, i-j; \Gamma^2 R_1 R_2) \quad (\text{A14})$$

$$[\hat{\rho}_{\mathcal{A}}^{1\psi}(T_1, T_2)]_{ijk}^{(i \leq j)} = \frac{1}{C^2} \Gamma^{i+k} (j+1)(j+k-i+1) \frac{T_1^{(i+k)/2} T_2^{(2j+k-i)/2} R_1^{j-i+1} \sqrt{j!(j+k-i)!}}{(j-i+1)! \sqrt{i!k!}} {}_2F_1(2+j, 2+j+k-i, 2+j-i; \Gamma^2 R_1 R_2) \quad (\text{A15})$$

According to previous considerations, the density matrices of the states $\hat{\rho}_{\mathcal{A}'}^0(T_1, T_2)$ and $\hat{\rho}_{\mathcal{A}'}^{1\psi_{\perp}}(T_1, T_2)$ for amplifier \mathcal{A}' can be directly derived from Eqs.(A8-A10) and (A13-A15) by substituting (Γ) with $(-\Gamma)$ and by relabelling the indexes describing the spatial and polarization modes. Finally, the complete output state can be reconstructed as:

$$\hat{\rho}^{1\psi}(T_1, T_2) = \hat{\rho}_{\mathcal{A}'}^{1\psi}(T_1, T_2) \otimes \hat{\rho}_{\mathcal{A}'}^0(T_1, T_2) \quad (\text{A16})$$

2. Density matrix coefficients on the reduced \mathbf{k}_1 spatial mode for the amplified states

In this section we report the expression of the coefficients for the reduced density matrix on spatial mode \mathbf{k}_1 of the $|\Phi^{1\psi}\rangle$ after the propagation over a lossy channel. Such result has been exploited in the calculation of the Bures distance, where the action of the O-Filter device

has been analyzed. The starting point of the calculation is the expression (A5) of the $|\Phi^{1\psi}\rangle$. After the partial trace on mode \mathbf{k}_2 , the density matrix $\hat{\rho}_{\mathbf{k}_1}^{1\psi} = \text{Tr}_{\mathbf{k}_2} [|\Phi^{1\psi}\rangle\langle\Phi^{1\psi}|]$ reads:

$$\hat{\rho}_{\mathbf{k}_1}^{1\psi} = \sum_{n=0}^{\infty} \sum_{m=0}^{\infty} \frac{\Gamma^{2n+2m}}{C^6} (n+1) |n+1\rangle\langle n+1| \otimes |m\rangle\langle m| \quad (\text{A17})$$

Finally, the application of the lossy channel map leads to the following density matrix:

$$\hat{\rho}_{\mathbf{k}_1}^{1\psi}(T) = \sum_{i=0}^{\infty} \sum_{j=0}^{\infty} \left[\rho_{\mathbf{k}_1}^{1\psi}(T) \right]_{ij} |i\rangle\langle i| \otimes |j\rangle\langle j| \quad (\text{A18})$$

where the coefficients are given by:

$$\left[\rho_{\mathbf{k}_1}^{1\psi} \right]_{ij} = \frac{\Gamma^{2i+2j-2}}{C^6} \eta^{i+j} (i + \Gamma^2(1-\eta)) (1 - \Gamma^2(1-\eta))^{-3-i-j} \quad (\text{A19})$$

-
- [1] E. Schrodinger, *Naturwissenschaften* **23**, 807 (1935).
 - [2] W. H. Zurek, *Rev. Mod. Phys.* **75**, 715 (2003).
 - [3] F. De Martini, F. Sciarrino, and C. Vitelli, *Phys. Rev. Lett.* **100**, 253601 (2008).
 - [4] W. Schleich, M. Pernigo, and F. Le Kien, *Phys. Rev. A* **44**, 2172 (1991).
 - [5] D. M. Greenberger, M. A. Horne, and A. Zeilinger, *Bell's theorem, Quantum Theory, and Conceptions of the Universe* (Kluwer Academic Publisher, 1989).
 - [6] F. De Martini, *Phys. Rev. Lett.* **81**, 2842 (1998).
 - [7] F. De Martini, *Phys. Lett. A* **250**, 15 (1998).
 - [8] E. Nagali, T. De Angelis, F. Sciarrino, and F. De Martini, *Phys. Rev. A* **76**, 042126 (2007).
 - [9] F. De Martini, F. Sciarrino, and N. Spagnolo, *Phys. Rev. A* **79**, 052305 (2009).
 - [10] F. De Martini, F. Sciarrino, and N. Spagnolo, *Phys. Rev. Lett.* **103**, 100501 (2009).
 - [11] F. De Martini and F. Sciarrino, *Progr. Quantum Electron.* **29**, 165 (2005).
 - [12] F. De Martini, F. Sciarrino, and V. Secondi, *Phys. Rev. Lett.* **95**, 240401 (2005).
 - [13] F. De Martini and F. Sciarrino, *J. Phys. A: Math. Theor.* **40**, 2977 (2007).
 - [14] D. Bures, *Trans. Am. Math. Soc.* **135**, 199 (1969).
 - [15] M. Hubner, *Phys. Lett. A* **163**, 239 (1992).
 - [16] R. Jozsa, *J. Mod. Opt.* **41**, 2315 (1994).
 - [17] D. Pelliccia, V. Schettini, F. Sciarrino, C. Sias, and F. De Martini, *Phys. Rev. A* **68**, 042306 (2003).
 - [18] F. De Martini, D. Pelliccia, and F. Sciarrino, *Phys. Rev. Lett.* **92**, 067901 (2004).
 - [19] F. De Martini, V. Buzek, F. Sciarrino, and C. Sias, *Nature* **419**, 815 (2002).
 - [20] A. Peres, *Quantum Theory: Methods and Concepts* (Kluwer Academic Publisher, 1995).
 - [21] B. Huttner, A. Muller, J. D. Gautier, H. Zbinden, and N. Gisin, *Phys. Rev. A* **54**, 3783 (1996).
 - [22] F. Sciarrino and F. De Martini, *Phys. Rev. A* **72**, 062313 (2005).
 - [23] F. Sciarrino and F. De Martini, *Phys. Rev. A* **76**, 012330 (2007).
 - [24] J. Cai, S. Popescu, and H.-J. Briegel, arXiv:0809.4906
 - [25] G.S. Engels, *et al.*, *Nature* **446**, 782 (2007)
 - [26] G. A. Durkin, C. Simon, J. Eisert, and D. Bouwmeester, *Phys. Rev. A* **70**, 062305 (2004).
 - [27] L. J. Slater, *Generalized Hypergeometric Functions* (Cambridge University Press, 1966).